DESIGN STUDY OF A 35.4 MeV CW DOUBLE-SIDED MICROTRON

T. Tanaka, K. Hayakawa, K. Tsukada, K. Sato, N. Nakamura, O. Takeda, M. Nishinaka
Atomic Energy Research Institute, Nihon University, Kanda-Surugadai, Chiyoda-ku, Tokyo, 101 Japan

Summary

A basic design study of a 35.4 MeV cw double-sided microtron (DSM) has been performed. A phase matching system is designed from an analysis of the longitudinal phase motion of an electron beam in acceleration. Parameters of a beam transport magnet system is determined by a calculation of a field strength distribution in sector magnets and first order calculation of beam optics.

Introduction

As a test machine for a one-GeV double-sided microtron for medical use[1], a 35.4 MeV cw double-sided microtron has been designed. This test machine will be helpful to reveal and improve possible technical problems such as alignment of magnets and accelerating tubes, beam blowup at high current acceleration and multi-recirculation, etc..

Design parameters of DSM are listed in table I. DSM is accompanied with a 5 MeV cw injector linac, which is also designed. A schematic layout of DSM is shown in fig. 1. The operating rf frequency of accelerating sections is 2398.34 MHz (wave length 12.5 cm). The disk-and-washer structure will be used for 2 m long accelerating tubes. The phase velocity of tubes will be chosen to be equal to the light velocity, c. The energy gain is 0.95 MeV/m at the nominal synchronous phase and 7.6 MeV per turn. The electron beam will be extracted at the energy of about 35.4 MeV after 4 turns. Details of design and calculations is discussed in the followings.

Longitudinal Phase Motion

The DSM mainly consists of two accelerating sections and four sector magnets. Focusing Q-magnets are placed between the sector magnets for each orbit and at the end of the accelerating sections. When extremely relativistic electrons are accelerated, the resonance condition is given as

$$(\pi-2)\frac{W_0\cos\phi_0}{ecB} = n\lambda, \qquad (1)$$

where $W_0\cos\phi_0$ is the energy gain per turn at the synchronous phase ϕ_0, B is the field strength of the sector magnets, λ (=12.5 cm) is the rf wave length and n is the mode number. In the present design n is chosen as unity. In order to obtain a constant energy gain in every turn, the electron energy E must satisfy the relation

$$(\pi-2)\frac{E}{ecB} + 2L_0 + L_1 = m\lambda\left(1+\frac{\theta}{2\pi}\right), \qquad (2)$$

where L_0 is the drift length between the accelerating sections and the sector magnets, L_1 is the distance between the two accelerating sections, m is a positive integer and θ is the rf phase difference between the two linacs. The drift length at both sides of the accelerating sections can be taken equal when the phase difference θ is chosen to be 90°.

The rf phase velocity is equal to c, while the velocity of the injected electrons is slightly lower

TABLE I

THE DSM DESIGN PARAMETERS

Injection energy	5 MeV
Extraction energy	35.4 MeV
Beam current	300 μA
Magnetic field	0.2315 T
Accelerating gradient	1.025 MeV/m
Nominal synchronous phase	22.05 deg.
Energy gain per turn	7.6 MeV
Number of turns	4
Operating rf frequency	2398.34 MHz
Accelerating tubes	2 m x 4
Rf power dissipation (inc. injector)	200 kW

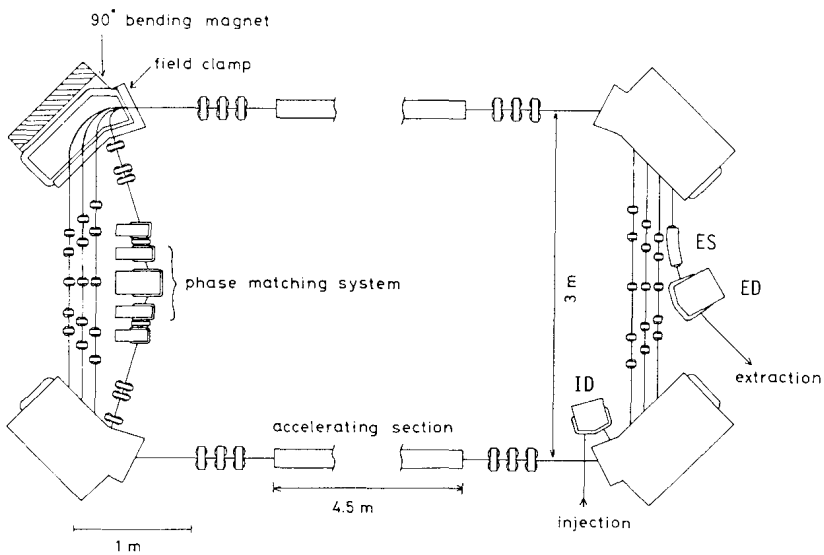

ID : 150° deflecting magnet
ED : 30° deflecting magnet
ES : 15° deflecting septum magnet

Fig. 1. Schematic layout of DSM. The electron beam is injected through deflections of 150° at the injecting magnet, ID and 120° at the sector magnet. The beam from the first accelerating section is deflected by 107° at the next sector magnet.

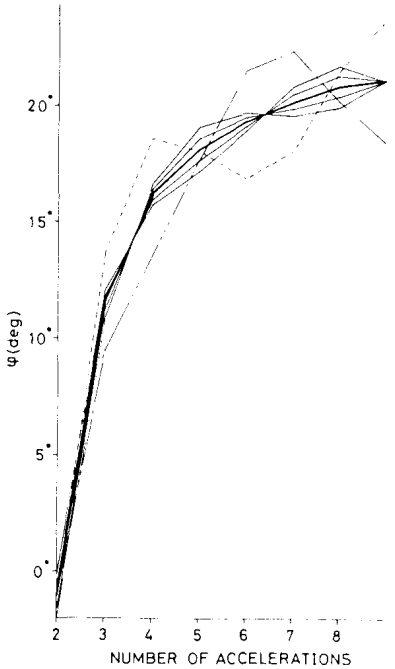

Fig. 2. The phase of beam bunches as a function of the number of accelerations. The central curve is for acceleration at the optimum phase. Also shown are the phase oscillations of bunches of ±0.5° and ±1° relative to the optimum phase (solid lines) and of ±50 keV relative to the optimum energy (broken line and dashed-dotted line) at the second acceleration.

than c, which causes a large phase slip of the electron bunch. The phase slip becomes small with increasing electron energy, and the bunch phase gradually becomes close to the synchronous phase, 22.05°. Therefore, the injection energy and phase must be different from nominal values. From a simulation of the phase slip, optimum values of the injection energy and phase have been deduced as 4.505 MeV and -50.975°, respectively. Fig. 2 shows the behaviour of the bunch phase during acceleration. The phase stability of the beam is also shown. In fig. 2, ϕ denotes the phase of the bunch at the entrance of the accelerating section. The injection phase is not plotted here. A large negative injection phase causes a transverse beam defocusing, which is due to the transverse component of the accelerating field. There is no focusing element in the accelerating sections. Therefore, the value $\phi = -50.975°$ is not suitable as an injection phase. In order to avoid such a large negative phase, a phase matching system is installed in the first shor straight section [1]. The 8.175 MeV electron beam is deflected by 107° at the sector magnet, then deflected by 17° in opposite direction so that the beam line becomes parallel to those of the regular shor straight sections. The orbit length can be controlled by changing the field strength of succeeding dipole magnets so that the bunch phase is adjusted to the optimum value at the entrance of the next accelerating section. The orbit length is a function of the injection energy and phase which give the electron energy of 8.175 MeV at the exit of the first accelerating section. The injection phase is -19.7° at the injection energy of 4.25 MeV and -3.3° at 4.50 MeV.

Design of Sector Magnets

The layout of the C-typed sector magnets is shown in fig. 1. The cross section is shown in fig. 3. The field distribution has been calculated from a two dimensional calculation code[2] TRIM. With the aid of an active field clamp, the equilibrium orbits outside of

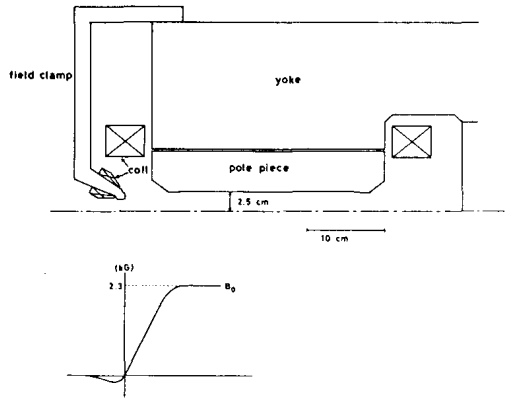

Fig. 3. Cross section of the sector magnet. Distribution of the vertical field at medium plane calculated by using TRIM is shown.

the magnet field can be adjusted to ideal orbits obtained from a shar cut off field approximation. This adjustment is important especially for orbits with small radii, since the electron beam must be re-injected to the central axis of the accelerating tubes. In order to obtain a uniform magnetic field in a wide range, a Purcell gap of 2.5 mm width is introduced between the pole piece and the return yoke. Also a shim is needed at the pole edge. As seen in fig. 1, the electron beam is injected to the first accelerating section after deflected by 150° at the injecting magnet and 120° at the sector magnet, then the beam from the first accelerating section is deflected by 107° at the next sector magnet. Therefore, the electron beam with low energy can experience the uniform field in the sector magnet owing to the particular shape of the field boundary. The vertical focusing effect in the fringing field has been simulated from the two dimensional field distribution. In this simulation, the rotation angle of the pole edges faced to the accelerating sections has been optimized to be 27°, so that the vertical defocus is suppressed in the short straight sections. The parameters of vertical focus obtained from the simulation is used for the calculation of the first order beam transfer matrices.

A model magnet is planned to be constructed for the study of the field uniformity, property of the active field clamp and the vertical focusing effect.

Beam Optics Calculations

The beam optics calculations have been performed on the basis of the first order beam matrix theory. The transverse beam emittances in both horizontal (x) and vertical (y) planes are assumed as $5/E\pi$ mm.mr. The energy spread is assumed as ±50 keV for all orbits.

Phase matching system

The 8.175 MeV electron beam from the first accelerating section is sequentially deflected by 107° and -17°, then transported to the phase matching system which consists of three dipole magnets. The 107° and -17° deflecting section forms an achromatic transport system. The three magnets are excited with the same field strength but the second magnet is excited reversely. The orbit in the second magnet is twice the length of those in the others. When the 4.25 MeV beam is injected in DSM, the orbit of 8.175 MeV transport line must be longer by 328.6° in rf phase angle than a regular 8.175 MeV line of 90° and 90° deflections. The orbit radius and deflecting angle in the first magnet have been adjusted so that the orbit length satisfies the above condition. The arrangement and the field strength of Q-magnets on the 8.175 MeV transport line have been determined by using the computer code[3] TRANSPORT. The

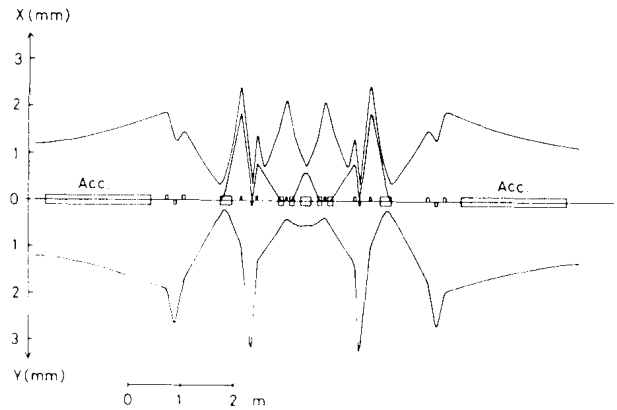

Fig. 4. The beam envelopes and the dispersion ray around the phase matching system. The energy spread is ± 50 keV. The beam sizes are 2.4 mm at the start point of calculation for both x and y planes.

beam envelopes in both horizontal and vertical planes are tuned symmetric about the midpoint of the second magnet. A waist to waist transformation is made between the midpoints of the accelerating sections. The beam diameters have been assumed as 2.4 mm at the initial waist. The result of calculation is shown in fig. 4, where both the horizontal and vertical beam envelopes and the horizontal dispersion ray are illustrated.

Short Straight Sections

Five Q-magnets are placed in each orbit of the short straight sections so that an achromatic transport system is formed. The beam envelopes in both horizontal and vertical planes are tuned symmetric about the midpoint of the short straight section[4]. The dispersion is chosen to be zero at the second and the fourth Q-magnets for easiness of beam control. When the second Q-magnet is placed nearer to the first one, the maximum horizontal size of the monochromatic beam can be more suppressed, while the dispersion becomes larger at the third Q-magnet. Such an arrangement will cause difficulties in machine operation if the beam energy is not adjusted suitably. Therefore, the distance between the first and the second Q-magnets has been chosen so that, at the expense of the beam size, the dispersion at the third Q-magnet does not exceed twice as large as that at

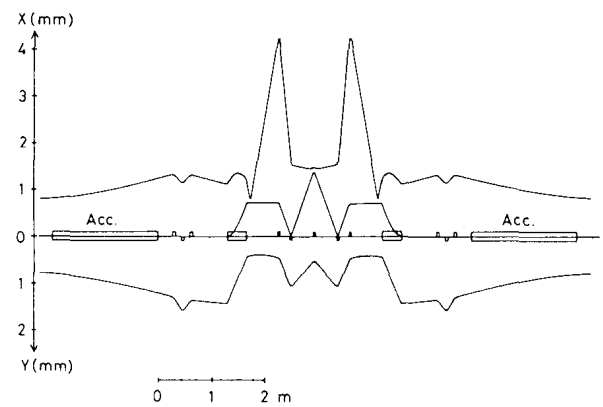

Fig. 5. The beam envelopes and the dispersion ray around the 16.146 MeV shor straight section. The beam sizes are 1.6 mm at the start point of calculation for both x and y planes. The energy spread is ± 50 keV.

the exit of the sector magnet. Fig. 5 shows the beam envelopes and the dispersion ray on the 16.146 MeV transport line. If the horizontal beam size should be more suppressed, one or two additional Q-magnets will be needed in the short straight section.

Quality of the Extracted Beam

The electron beam is extracted from DSM with the energy of 35.338 MeV, which has been resulted from the simulation of the phase slip. The transverse emittances of the extracted beam are expected to be 0.14π mm·mr in both the horizontal and the vertical planes if the emittances are expressed as 5/Eπ mm·mr. The energy spread of the extracted beam depends on the accelerating gradient, the synchronous phase and the shape of the longitudinal phase ellipse at the injection point. From a result of simulation, a narrow ellipse is desirable in order to obtain a beam with a sharp energy spectrum. Fig. 6 shows the change of the longitudinal phase space distribution of the beam from 8.175 MeV to 35.338 MeV, where the initial conditions at the injection point are $\Delta\phi = \pm 0.5°$ and $\Delta E = \pm 50$ keV. The injector linac and the injection transport system will be designed in consideration of the above conditions.

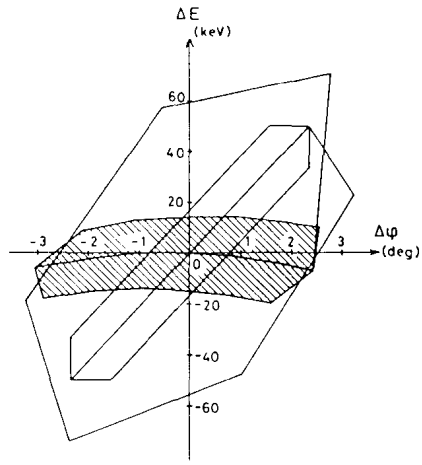

Fig. 6. The behaviour of the longitudinal phase space distribution of the beam around the optimum phase and energy. The relation of the distributions between 8.175 MeV (not hatched) and 35.338 MeV (hatched) is illustrated. The initial conditions at the injection point are $\Delta\phi = \pm 0.5°$ and $\Delta E = \pm 50$ keV.

References

1. K. Hayakawa et al., IEEE Trans. Nucl. Sci. NS-30, 4, 3224 (1983).
2. J.S. Colonias, UCRL-18439 (1968).
3. K.L. Brown et al., SLAC-91 (1974).
4. H.E. Jackson et al., ANL-82-22 (1982).